



1 **Advection (non-climate) impact on the South Pole Ice Core**

2 Tyler J. Fudge¹, David A. Lilien^{1,2}, Michelle Koutnik¹, Howard Conway¹, C. Max Stevens¹,

3 Edwin D. Waddington¹, Eric J. Steig¹, Andrew J. Schauer¹

4 ¹ Earth and Space Sciences; University of Washington, Seattle, WA 98195

5 ² Physics of Ice, Climate, and Earth; Niels Bohr Institute, Copenhagen, Denmark

6 Email correspondence: tjfudge@uw.edu

7

8



9 **Abstract**

10 The South Pole Ice Core (SPICEcore), which spans the past 54,300 years, was drilled far from an
11 ice divide such that ice recovered at depth originated at a location upstream of the current core
12 site. If the climate is different upstream, the climate history recovered from the core will be a
13 combination of the upstream conditions advected to the core site and the temporal changes we
14 seek to recover. Here, we evaluate the impact of ice advection on two fundamental records from
15 SPICEcore: accumulation rate and water isotopes. We determined the past locations of ice
16 deposition based on GPS measurements of the modern velocity field spanning 100km upstream
17 where ice of ~20 ka age would likely have originated. Beyond 100km, there are no velocity
18 measurements, but ice likely originates from Titan Dome, an additional 90km distant. Shallow
19 radar measurements extending 100km upstream from the core site reveal large (~20%) variations
20 in accumulation but no significant trend. Water isotope ratios, measured at 12.5km intervals for
21 the first 100km of the flowline, show a decrease with elevation (and distance upstream) of -
22 0.008‰ m⁻¹ for δ¹⁸O. Advection therefore adds approximately 1‰ for δ¹⁸O to the LGM-to-
23 modern change. Assuming a lapse rate of 10°C per km of elevation, the LGM-to-modern
24 temperature change is ~1.5°C greater than if the ice had been deposited at a fixed location.

25

26



27 **Introduction**

28 Ice cores provide unique and detailed records of past climate (e.g. Alley et al., 1993; Petit et al.,
29 1999; NorthGRIP, 2004; Marcott et al., 2014). Such records are most useful if they represent the
30 change in climate at a fixed geographic location and elevation. Two important non-climatic
31 influences on ice core records are changes in ice-sheet elevation (Vinther et al., 2009; Steig et al.,
32 2001; Stenni et al., 2011; Parennin et al., 2007; Cuffey and Clow, 1997) and changes in the
33 location of ice origin due to flow (Whillans et al., 1984; Huybrechts et al., 2007; NEEM, 2013;
34 Steig et al., 2013; Koutnik et al., 2016). Many ice cores are drilled near an ice divide to minimize
35 both of these effects: ice thickness changes less in the interior than on the margins (Cuffey and
36 Paterson, 2010) and there is little lateral ice flow near a divide. The change in ice thickness can
37 be evaluated with ice-flow models (Parrenin et al., 2007; Golledge et al., 2014; Briggs et al.,
38 2014) or measurements from the ice core itself (Martinerie et al, 1994; Steig et al., 2001; Vinther
39 et al., 2009; Waddington et al., 2005; Price et al., 2007). The focus of this work is the impact of
40 ice flow on the South Pole Ice Core (SPICEcore). We will use the term “advection impact” to
41 refer to the variations in the ice-core histories that are due to deposition upstream in different
42 climate conditions, as opposed to temporal changes in the climate at the ice-core site.

43

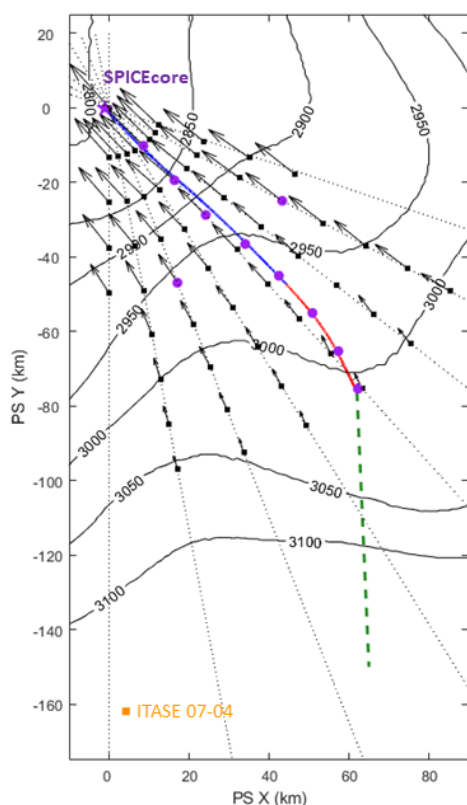
44 Ice cores are often drilled far enough from divides that lateral advection is important because of
45 site characteristics (NorthGRIP, 2004; EDML, EPICA 2006; WAIS Divide, Morse et al., 2005;
46 NEEM, 2013), logistical considerations (Camp Century, Gow et al., 1968; Dye-3, Dansgaard et
47 al., 1969; Byrd, Hammer et al., 1980; Vostok, Lorius et al., 1985), or concern about divide
48 migration over the drill site (Waddington et al., 2001). The importance of advection on ice core
49 records depends on both the velocity of the ice and the gradient in the parameter of interest. For
50 well-mixed atmospheric gases, such as carbon dioxide and methane, there is no direct impact on
51 the histories. Instead, the affected histories are primarily those recovered from the ice phase:
52 accumulation rate, water isotopes, surface temperature, and aerosols. Of the cores that have been
53 drilled away from ice divides, the horizontal velocities range from approximately 1 m a^{-1}
54 (EDML) to 12 m a^{-1} (Dye 3) and all require correction to obtain the climate history for a fixed
55 geographic location (Whillans et al., 1984; Steig et al., 2001; Huybrechts et al., 2007; Vinther et
56 al., 2009; NEEM, 2013; Steig et al., 2013; Koutnik et al., 2016).

57



58 The 1750 m long SPICEcore was obtained at the South Pole between 2014 and 2016.
59 SPICEcore was sited, in part, to take logistical advantage of South Pole station where the surface
60 velocity is 10 m a^{-1} in the direction of 40°W (Hamilton, 2004; Casey et al., 2014). Lilien et al.
61 (2018) inferred the flowline out to 100 km upstream and concluded that Titan Dome is the likely
62 source region for ice reaching the SPICEcore site. Previous measurements of water isotope
63 values upstream of South Pole are primarily from surface snow samples, which do not provide
64 reliable time-averaged values (Masson-Delmotte et al., 2008; Dixon et al., 2013). A shallow ice
65 core near Titan Dome (US-ITASE 07-4) provides a single estimate of accumulation (0.074 m ice
66 equivalent a^{-1} ; Dan Dixon, personal communication). Here, we assess the advection impact on
67 the accumulation-rate, water-isotope, and surface-temperature histories of SPICEcore using new
68 measurements in the upstream catchment.

69



70

71

72 Figure 1: Map of the area upstream of
73 the South Pole. SPICEcore location is
74 purple star. 10m core locations are
75 purple circles. Stake locations (black
76 squares) were surveyed with GPS and
77 plotted with velocity vectors. Flowline
78 was inferred from the velocity
79 measurements for past 10 ka (blue, from
80 Lilien et al., 2018) and 10 ka to 21 ka
81 (red). Unconstrained flowline for 21 ka
82 to 55 ka is dashed green. Surface
83 topography contours are from BedMap2
84 (Fretwell et al., 2013). ITASE 07-04
85 core at Titan Dome is orange square.
86 Note that Titan Dome is a broad ridge
87 and the geometry is not well defined in
88 BedMap2 and the elevation does not
89 match the 3090 m measured by Dixon
90 et al. (2013).



91 **Methods**

92 To assess the impact of advection on the SPICEcore climate histories, we measured ice velocity,
93 accumulation rates, water isotopes, and firn temperatures in the upstream catchment. The surface
94 ice-flow velocities, inferred flowline, and spatial pattern of accumulation were described by
95 Lilien et al. (2018; <http://www.usap-dc.org/view/dataset/601100>) and we provide only a brief
96 review below.

97

98 *Surface Ice-flow Velocity and Flowline Determination*

99 Determining the ice-flow velocity near South Pole is more difficult than many other
100 locations in Antarctica; there is little satellite coverage due to the geometry of satellite orbits
101 which creates a “pole hole.” Rignot et al. (2011) used synthetic aperture radar to compute the
102 surface velocity, but utilized a substantially tilted satellite view, resulting in velocity
103 measurements that are not sufficiently precise to define the flowline. To obtain improved
104 velocity measurements in the region, we performed repeat surveys of stakes with GPS during
105 four consecutive field seasons. We installed 56 stakes at 12.5km intervals along lines of
106 longitude from 110°E to 180°E at 10° intervals (Lilien et al., 2018). The 110° and 180° lines
107 were measured only to 50 km from South Pole; the others were measured to 100 km (Figure 1).
108 The measured velocities range from 3 to 10 m a⁻¹, with errors of ±0.02 to 0.25 m a⁻¹ in each
109 horizontal direction. We used the measured velocity field to determine the modern flowline.
110 Starting at the SPICEcore drill site, we recursively stepped upstream in one-year intervals in the
111 direction opposite the velocity vectors to obtain annual positions along the flowline. We assume
112 that the surface velocity is constant for the upper 1750m of the ice column (the depth of
113 SPICEcore), because the warmer ice below 1750m contributes nearly all of the deformation
114 driving the surface velocity.

115

116 *Accumulation*

117 The accumulation rate along the flowline is derived from radar layers imaged from
118 approximately 20 m to 100 m depth with a 200 MHz radar (details can be found in Lilien et al.,
119 2018). The depth of a radar layer is converted to an accumulation rate using the density profile
120 and depth-age relationship of a core drilled on the flowline 50 km upstream from SPICEcore.
121 The firn depth-density profile is assumed to be unchanging along the flowline. The firn density



122 affects the derived accumulation rate history both through the inferred depth of the layer due to
123 the radar-wave propagation speed and through the conversion to ice-equivalent thickness. These
124 two uncertainties oppose each other but do not necessarily cancel. Using four additional density
125 profiles near South Pole, Lilien et al. (2018; Figure S4) found the spread in accumulation has a
126 standard deviation of 2.3% for a layer at ~20m depth. Deeper layers have a smaller spread
127 because the density is most variable near the surface. All accumulation rates are given in m a^{-1} of
128 ice equivalent.

129

130 *Water Isotopes*

131 Water isotopes ratios of $\delta^{18}\text{O}$ and δD were measured in cores of approximately 10 m depth at
132 12.5 km spacing along the flowline, as well as at two sites 15 km perpendicular to the flowline
133 50 km upstream of SPICEcore, for a total of 10 firn cores. We also report the deuterium excess,
134 using the log definition (d_{in} ; Markle et al., 2017). The cores were sampled at 0.5 m intervals in
135 the field and allowed to melt in plastic bottles. The measurements were performed at the
136 University of Washington's Isolab with a Picarro L-2120i. The average $\delta^{18}\text{O}$ and δD values (vs
137 Vienna Standard Mean Ocean Water) for each core are presented here. The cores were not dated
138 and thus the water isotopes cannot be averaged over the same ages; averaging using only the
139 upper 5 m for each core instead of the full core produced negligible differences. One outlier from
140 0.5-1 m depth at site 25km was excluded.

141

142 *10 m Temperatures*

143 The temperature at approximately 10 m depth was measured in each borehole left by the
144 shallow-core extraction. We averaged the values measured by four thermistors surrounded by a
145 copper shield. The thermistors were left in the borehole for different lengths of time ranging
146 from 28 minutes to 48 hours.

147

148 **Results**

149 **Gradients in Upstream Climate Parameters**

150 *Accumulation*

151 The accumulation rate along the 100 km flowline for four different internal layers is shown in
152 Figure 2. The youngest layer is 151 years before 2017 (~20m depth) and was used by Lilien et al.



153 (2018); the 743-year layer is the deepest (~90 m) layer resolved. Although the layers are
154 relatively young, there can still be a horizontal offset of hundreds of meters to kilometers from
155 where the layer was deposited on the surface. In Figure 2A, the accumulation rates in the upper
156 panel are plotted at the position of the radar trace. The impact of horizontal advection can be
157 observed as the older layers appear shifted to left (closer to SPICEcore) compared to the younger
158 layers.

159

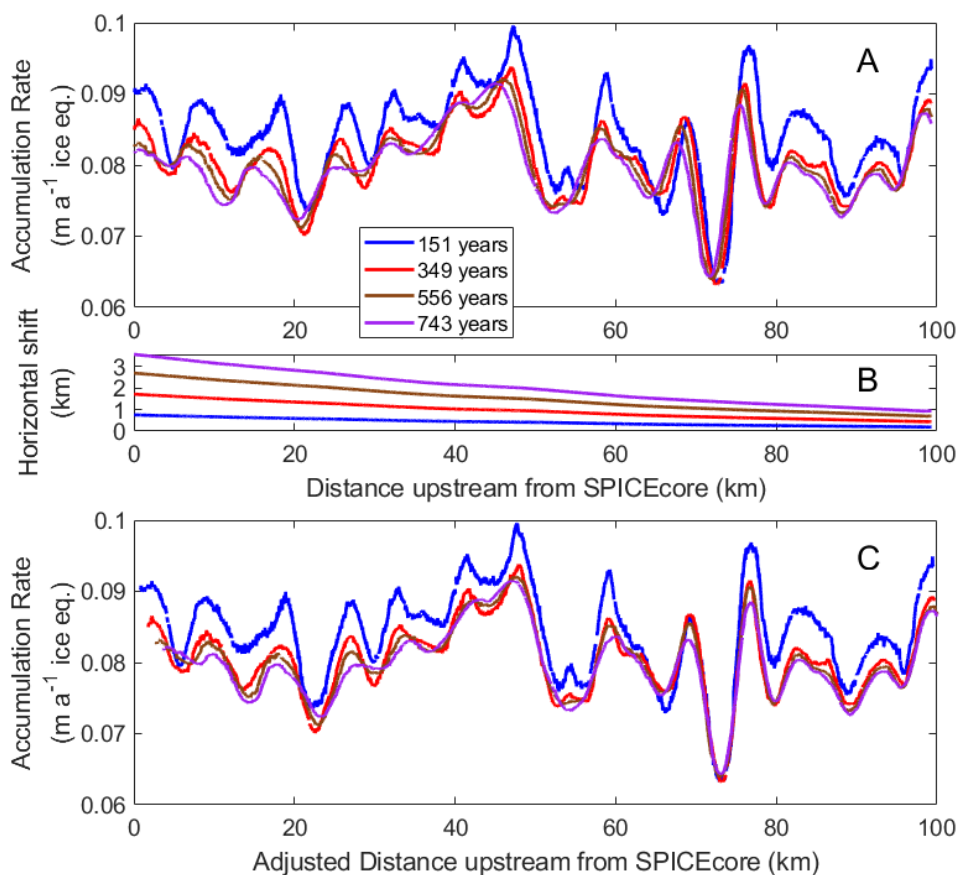
160 To account for horizontal advection, the position where the accumulation rate is inferred (i.e. the
161 location of the radar trace) is adjusted. This adjustment is made by multiplying the half-age of
162 the layer by the surface velocity at the mid-point of its path from deposition to the current trace
163 location (Figure 2B). The adjustment ranges from 3.7 km at SPICEcore for the 743-year layer to
164 0.2 km for the 151-year layer at the upstream end. Shifting the distance of the accumulation
165 records (Figure 2C) better aligns the peaks and troughs among the four layers. It also highlights
166 that older layers vary less along flow. The depth of a layer reflects the average surface
167 accumulation rate over the distance traveled. Thus, an older layer is flatter because it averages
168 the influence of accumulation on vertical velocity over a longer distance. This shows that simply
169 shifting the position of the layers to account for horizontal advection does not fully recover the
170 spatial variations in accumulation.

171

172 A more-complete treatment could solve an inverse problem to infer the surface accumulation rate
173 along the flow line that best matches the observed layer thicknesses (e.g., Waddington et al.,
174 2007). We do not address this problem here because we focus on the advection impact on the
175 SPICEcore record and not a formal evaluation of the surface accumulation patterns consistent
176 with available layers. Lilien et al. (2018, supplement) showed that the 151-year layer was
177 sufficiently deep to record real climate variations, and not noise, but shallow enough to not be
178 significantly affected by lateral flow.

179

180



181

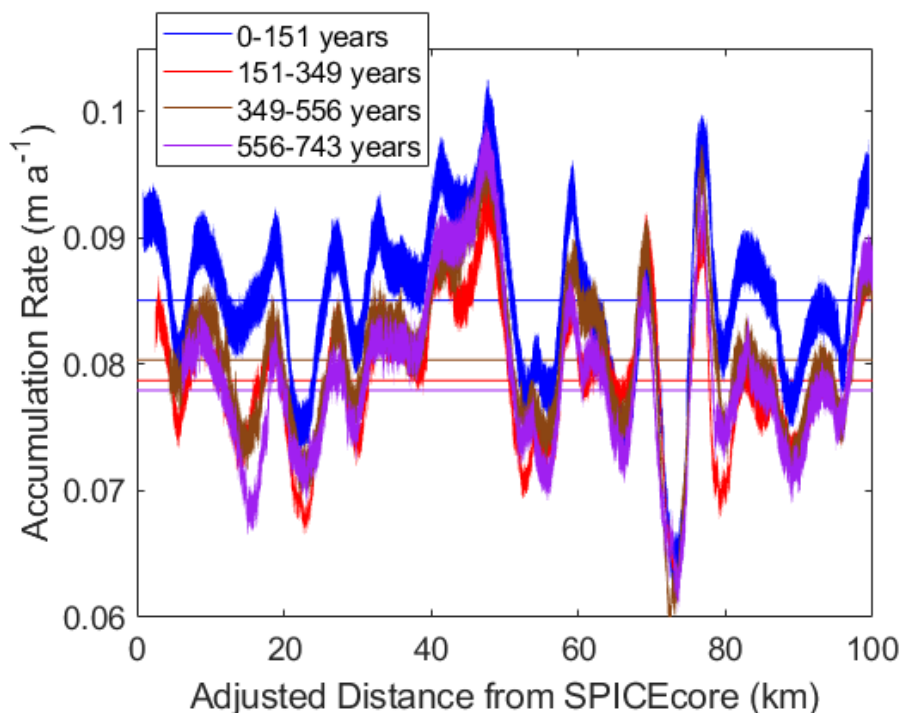
182 Figure 2: **Accumulation rate along flowline.** Panel A shows the accumulation rate for four
183 radar layers, with ages in years before 2017. Panel B shows average horizontal distance traveled.
184 Panel C shows same inferred accumulation as in Panel A, except the position is adjusted to
185 account for the horizontal distance traveled.

186

187 The average accumulation rate of the oldest (743-year-old) layer is 0.080 m a^{-1} and there is a
188 negligible spatial linear trend of $-4 \times 10^{-6} \text{ m a}^{-1} \text{ km}^{-1}$. The spatial variations are approximately
189 $\pm 20\%$ compared to the average value, much larger than the linear trend. Beyond the 100 km of
190 mapped flowline, the only accumulation-rate information is from the US-ITASE 07-04 core near
191 Titan Dome, where an accumulation rate of 0.074 m a^{-1} was inferred (Daniel Dixon, personal
192 communication, 2013). This is within the range of accumulation rates identified along the



193 flowline, but it is smaller than the 0.080 m a^{-1} average along the first 100km of the flowline.
194 With only a single point measurement, we cannot resolve whether this accumulation rate near
195 Titan Dome is representative of a mean value for a wider area.
196
197 We also calculate the accumulation rate for the intervals between successive layers (Figure 3)
198 which allows temporal trends to be more clearly evaluated. The uncertainty in the accumulation
199 rate is greatest for the 151-year layer because the density measurements are least certain in the
200 lower-density surface snow, and surface firm conditions are more spatially variable. We calculate
201 the uncertainty for an interval based on the density profiles of five different firm cores (the core
202 we drilled at 50km and four cores from near South Pole; Severinghaus et al., 2001; Christo
203 Buizert, personal communication). The uncertainty shading shown in Figure 3 is the range
204 between the maximum and minimum accumulation rates using the five density profiles. The
205 spatial average of the three older intervals are within uncertainty of each other. The spatial
206 average of the 0 to 151-year interval is always greater than the older three intervals. Because the
207 spatial average of the minimum accumulation rate (based on firm density) for 0 to 151-year is
208 greater than the spatial average of the maximum for the older intervals, we have confidence that
209 the accumulation rate has increased in the past 151 years. The accumulation increase is $8 \pm 4\%$
210 compared to the previous 592 years (151 to 743 years before 2017).
211



212

213 Figure 3: Temporal average accumulation rate for ages between radar layers. Shading indicates
 214 uncertainty based on five firn-density profiles. Distance from SPICEcore has been adjusted as in
 215 Figure 2 and described in main text. Horizontal lines indicate spatial average of the accumulation
 216 rate using the density profile measured on the firn core at 50km.

217

Table 1: Accumulation Increase in past 151 years relative to previous periods

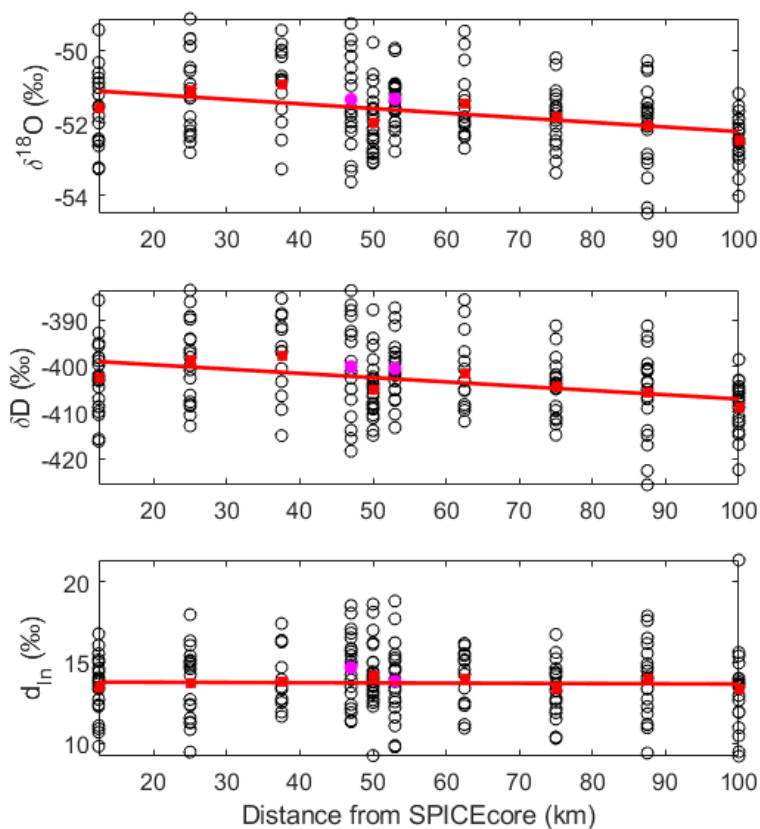
Interval	Mean	Minimum	Maximum
151-349	8%	4%	12%
349-556	6%	1%	11%
556-743	9%	3%	13%
151-743	8%	4%	12%

Mean increase uses density profile from the core at 50km for all layers
 Minimum (maximum) increase uses density profile which yields the minimum (maximum) accumulation rate
 for the 0-151 interval and the density profile which yields the maximum (minimum) for the older layers.



218 *Water Isotopes*

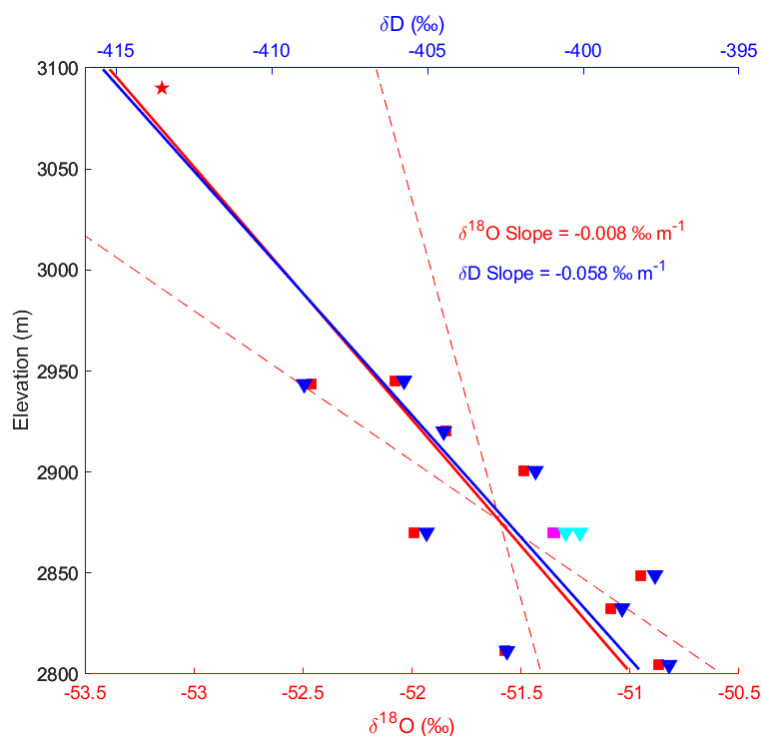
219 Measurements of water isotopes require the collection of ice samples and thus have much more
220 limited spatial resolution than the accumulation-rate measurements. There is considerable scatter
221 (Figure 4) in the 0.5 m resolution samples, which have durations of a few years of time (i.e. 2-4
222 years) per sample; the differences among 0.5 m samples are likely driven by interannual
223 variations. Using the mean values, a decrease with distance from South Pole is observable in
224 both $\delta^{18}\text{O}$ and δD . The d_{in} values show no significant trend upstream.
225



226
227 Figure 4: Water-isotope values (black circles) and averages (red squares) for shallow cores along
228 the flowline upstream of South Pole. Cores at 50km upstream on 120E and 160E are plotted at
229 47km and 53km (magenta circles). Linear slope (thick red line) is from the average values along
230 the flowline only.



231 The $\delta^{18}\text{O}$ and δD values are also shown in Figure 5 but are plotted by elevation rather than
232 distance upstream. Linear fits to $\delta^{18}\text{O}$ and δD yield slopes of $-0.0080 \pm 0.0055 \text{‰ m}^{-1}$ and -
233 $0.0579 \pm 0.04 \text{‰ m}^{-1}$ respectively (95% confidence levels). Including the average $\delta^{18}\text{O}$ value
234 from the upper 1.2m of the firn core at Titan Dome (-53.15‰) in the linear regression changes
235 the slope to -0.0073‰ m^{-1} , which is in good agreement with the mean slope. Because the Titan
236 Dome value is an average of only the upper 1.2m and not directly comparable in time to our
237 10m-average measurements, we use the mean slope of 0.008‰/m^{-1} from the 10m cores for the
238 advection correction described in the subsequent section.

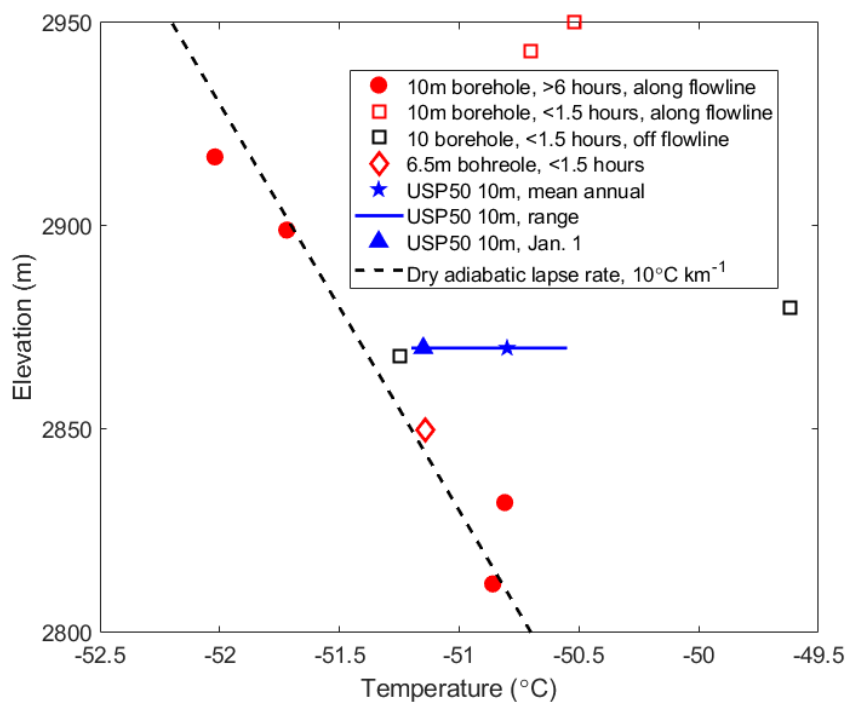


239
240 Figure 5: Average $\delta^{18}\text{O}$ (red squares) and δD (blue triangles) values from the 10m cores along
241 the flow line and SPICEcore. Average $\delta^{18}\text{O}$ and δD from cores off of the flowline at 50km
242 upstream (pink squares and cyan triangles). $\delta^{18}\text{O}$ of US-ITASE 07-04 core at Titan Dome (red
243 star). Linear fit of 10m cores along the flow line for $\delta^{18}\text{O}$ (red thick line) and δD (blue thick line)
244 do not include Titan Dome or cores from off the flowline. 95% confidence intervals of the $\delta^{18}\text{O}$
245 fit (red dashed lines) are shown. Confidence intervals of δD overplot those of $\delta^{18}\text{O}$ and are not
246 shown.



247 *Surface Temperature Gradient*

248 The ~10 m temperatures are shown in Figure 6. Unfortunately, a variety of differences in the
249 measurement procedure were made because of time constraints of the field work, and these
250 prevented a determination of the gradient in mean annual temperature. Based on cooling curves
251 (not shown) from two boreholes, measurements that equilibrated for less than 1.5 hours yielded
252 warmer temperatures than those left in boreholes for longer times, and we consider those
253 measurements less reliable. Measurements that were made after leaving the thermistors in the
254 boreholes for longer than six hours are consistent with a dry adiabatic lapse rate of $10^{\circ}\text{C km}^{-1}$,
255 but we cannot reject a wide range of other values for the lapse rate.



256
257 Figure 6: Temperature measurements. Filled symbols equilibrated for more than 6 hours; open symbols
258 equilibrated for less than 1.5 hours. Red symbols are along the flow line; black symbols are off the
259 flowline. Diamond is a measurement at 6.5 m depth, which is likely $\sim 0.7^{\circ}\text{C}$ colder due to the winter cold
260 wave than if measured at 10 m depth. Blue symbols are from a single thermistor installed at 10 m depth in
261 a back-filled borehole with measurements recorded more than 1 year; star is mean annual temperature,
262 triangle is initial temperature after equilibration and horizontal line is the range of temperature recorded.
263 Black dashed line shows a lapse rate of $10^{\circ}\text{C km}^{-1}$.



264 **Determination of Flowline Position and Age**

265 The location where ice in SPICEcore fell on the surface is well constrained for the past 10 ka by
266 Lilien et al. (2018). For ice older than 10 ka, the spatial variations in the accumulation rate
267 cannot be clearly correlated with the layer thickness variations in SPICEcore. This is likely
268 because: 1) uncertainty in the flowline position accumulates with distance (age); 2) the relative
269 uncertainty in the surface velocity increases as the velocity decreases with distance upstream; 3)
270 the surface-velocity measurement stakes are farther apart; and 4) the temporal variations in
271 accumulation are likely larger during the isotopic maximum at ~11 ka and the glacial-interglacial
272 transition (Veres et al., 2013; Fudge et al., 2016).

273

274 We divide the reconstruction of the flowline into three segments based on the data available. The
275 first segment is the flowline inferred by Lilien et al. (2018) which includes the inference of a
276 15% speed-up during the past 10 ka. The first segment covers 70 km from SPICEcore.

277

278 The second segment of the flowline spans from 70 km to the limit of the surface velocity
279 measurements at 100 km from the SPICEcore drill site. To determine the flowline, we assume
280 that the direction of ice flow was not different than what is measured today. We also assume the
281 15% lower velocity at 10 ka found by Lilien et al. (2018) is appropriate for older ages. We
282 recognize that velocity changes during the glacial-interglacial transition, when the accumulation
283 rate roughly doubled, are likely; however, it is unclear what the effect is for this region. If the
284 velocity was determined by the amount of accumulation (i.e. balance velocity), we might expect
285 the 20 ka speed to be approximately half of the 10 ka speed, mirroring the glacial-interglacial
286 change in accumulation rate. However, results from a full ice-sheet model (Pollard and DeConto,
287 2009) show surface velocities 20% faster at 20ka compared to 10 ka. On the other hand, an
288 updated version of the same model (Deconto and Pollard, 2016), shows 25% slower velocities at
289 20 ka compared to 10 ka. Since there is no unambiguous estimate of velocity change during the
290 glacial-interglacial transition, we make the simplest assumption of holding the inferred 10 ka
291 velocity constant for older ages. Thus, ice of 21.6 ka age would have originated 100km from
292 SPICEcore with older ice originating beyond the measured flowline.

293



294 For ice in SPICEcore with ages older than 21.6 ka, no surface-velocity measurements exist to
295 help define where the ice originated. We examined the utility of the surface topography (Fretwell
296 et al., 2013) in defining the flow direction by tracking particles along the steepest descent. We
297 computed two flowlines, one stepping upstream from SPICEcore and the other stepping
298 downstream from the 10 ka location. They do not agree with each other or with the measured
299 flowline, which is not surprising given the limited data in the surface DEM and the convergent
300 flow. Thus, we cannot expect the surface topography to be useful in defining the x and y
301 components of the flowline beyond 100km. Therefore, we neglect variations in the direction of
302 flow and assume that the ice has flowed in a straight line from an ice divide (Figure 1). The
303 position of the ice divide is not well defined and we assume it is an additional 90km distant. We
304 also assume that the velocity decreases linearly from its value at 100km to zero at the divide,
305 which is equivalent to assuming a balance velocity in an ice sheet with uniform ice thickness and
306 accumulation rate and no convergence or divergence. These assumptions suggest the oldest
307 SPICEcore ice (54.3 ka) originated ~35km downstream from the assumed divide position.

308

309 **Advection Impact**

310 The advection impact on the SPICEcore accumulation-rate and water-isotope histories are quite
311 different from one another. The accumulation rate is sampled with high frequency but shows no
312 long-term trend with distance and elevation. The water isotopes, on the other hand, are sampled
313 infrequently but show a linear trend with distance and elevation. We discuss the advection
314 impact for the two separately.

315

316 *Accumulation Rate*

317 The lack of a linear trend in the accumulation rate along the flowline indicates that no trend
318 should be removed from the SPICEcore accumulation history. However, the variation in
319 accumulation upstream has a major impact on the SPICEcore history. Lilien et al. (2018) were
320 able to isolate the influence of km-scale upstream variability for the past 10 ka, which explains a
321 majority of the variance in the SPICEcore accumulation history. Thus, little of the variability in
322 the accumulation history for the past 10 ka is due to climate. While the residual variance of the
323 SPICEcore accumulation history (the accumulation history after removing the advection impact)
324 might reflect temporal changes in climate, the residual variance is also affected by multiple



325 sources of uncertainty such as the assumptions of a constant spatial pattern of accumulation, a
326 fixed flowline, a linear speed up, and a spatially homogeneous firn-density profile. These
327 uncertainties are sufficiently large and difficult to quantify that we do not interpret the residual as
328 a temporal history of accumulation.

329

330 Beyond 10 ka, it is important to understand the potential influences of spatial variations in order
331 to avoid erroneous conclusions about temporal variations in the accumulation rate over the past
332 55 ka. Since there is no overall trend, we are primarily interested in how the spatial variability
333 could be imprinted in the ice-core history. Spectral analysis shows that there is significant power
334 at a wavelength of 5 to 10 km. The temporal imprint of the spatial variations is then determined
335 by the ice-flow velocity, which is 4 m a^{-1} for ice of 10 ka age and decreases to 1 m a^{-1} for ice of
336 55 ka age. The timescales affected in the accumulation history are ~1 to 3 ka during the deglacial
337 transition (10-20 ka) and get longer, reaching 10 ka, for the oldest SPICEcore ice. The advection
338 impact on the deglacial transition may affect the specific timing of accumulation-rate change, but
339 not the overall temporal trend. For older ages, the advection impact has a similar timescale to
340 millennial-scale climate variations. We thus expect that the advection impact will decrease the
341 coherence between the accumulation-rate history and the temperature history inferred from water
342 isotopes.

343

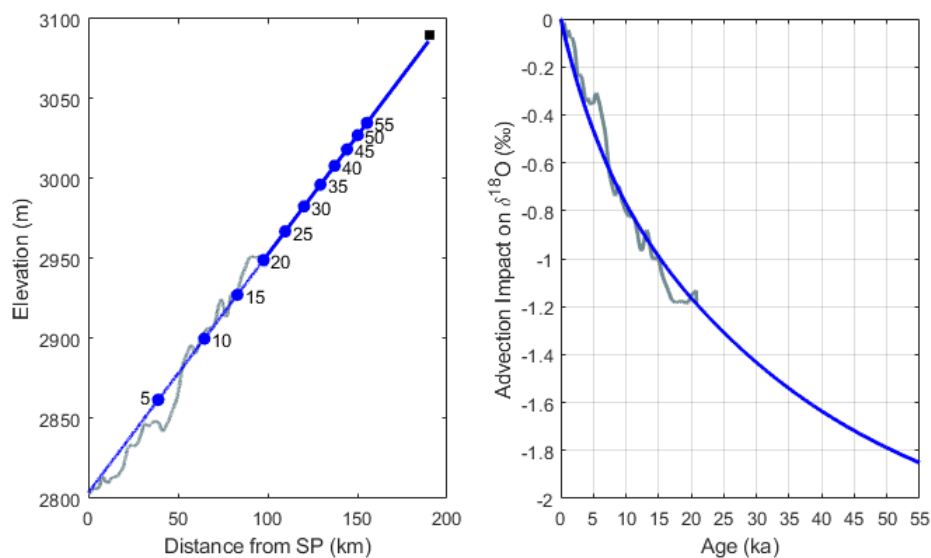
344 *Water Isotopes*

345 The water isotopes are not sampled at a high enough spatial resolution to perform an analysis of
346 millennial-scale variations as was done for the accumulation rate; however, the $\delta^{18}\text{O}$ and δD both
347 show linear trends with elevation and distance. Because $\delta^{18}\text{O}$ and δD are similar, we will discuss
348 only the advection correction for $\delta^{18}\text{O}$ in this section (both are provided in the supplemental
349 spreadsheet). A correction for advection becomes important, particularly for questions such as
350 the magnitude of the glacial-interglacial change. We use a linear fit to elevation data as the base
351 for the advection correction (Figure 7). The linear fit is continued beyond 100km at the same
352 slope, reaching an elevation similar to the US-ITASE 07-04 core at 190km upstream of
353 SPICEcore. We use the linear fit to avoid meter-scale elevation variability being added through
354 the advection correction.

355



366 The advection correction reaches a maximum of -1.7‰ at 54 ka. A negative value indicates the
367 ice recovered in the core fell at a location where the water isotopes are more depleted than at
368 South Pole in the current climate. Thus, the SPICEcore ice at 54 ka would be 1.7‰ more
369 enriched if it had fallen at South Pole instead of ~ 150 km upstream at ~ 220 m higher elevation.
370 Because the elevation change is linear with distance, the curvature of the advection impact is
371 determined by the change in ice velocity and the advection impact increases the most rapidly at
372 the youngest ages. The difference over the Holocene (past 10 ka) is 0.7‰ while the difference
373 over the previous 10 ka (10 to 20 ka) is 0.36‰ . The advection impact for the oldest ice is only
374 about 0.1‰ per 10 ka. Overall, the impact on the LGM-modern change is a little more than 1‰
375 compared to modern, although only about 0.6‰ compared to mid-Holocene values (i.e. 5 ka).



367
368 Figure 7: Advection Impact for $\delta^{18}\text{O}$. Left Panel: Elevation profile (gray) and linear fit (blue) used in
369 advection correction. Elevations at 5 ka intervals shown by blue dots.
370 Right panel: Advection correction using elevations in left panel. Blue is smooth (linear elevation)
371 correction; gray is if the modern, measured elevations were used. A negative value indicates the ice
372 recovered in the core fell at a location where the water isotopes are more depleted than South Pole in the
373 current climate.
374
375



376 **Discussion**

377 Advection has enhanced the glacial-interglacial $\delta^{18}\text{O}$ change at SPICEcore by 1‰ because ice in
378 the core originated at higher elevations with more depleted isotopic values. The total LGM (18 to
379 22 ka) to modern (past 1 ka) $\delta^{18}\text{O}$ change is approximately 6‰ (Steig et al., in prep.).

380 Accounting for advection reduces the fixed-location glacial-interglacial change to 5‰.

381 Advection has the opposite impact at WDC, where advection increases the glacial-interglacial
382 change by 1‰ (Steig et al., 2013), to 8‰. Understanding the advection impact is important for
383 comparing the magnitude of isotopic change among Antarctic ice cores; WDC has a 1‰ greater
384 LGM-modern change than SPICEcore in the raw records, but a 3‰ greater change after
385 accounting for advection. Because SPICEcore and WDC have similar source regions and
386 distillation pathways (e.g. Sodemann and Stohl, 2009), the difference between the two cores has
387 the potential to yield insight into relative elevation change between the West and East Antarctic
388 ice sheets. A full interpretation of relative isotopic change between SPICEcore and WDC is
389 beyond the scope of this paper, but the advection impact is a critical input for future analysis.

390

391 The advection impact on the accumulation history is distinct from that for the water isotopes.

392 There is no linear trend in accumulation in the upstream catchment, and thus no trend to remove
393 from the SPICEcore accumulation history. However, high spatial resolution of the modern
394 upstream accumulation pattern has revealed that the majority of the accumulation variability in
395 the past 10 ka (Lilien et al., 2018) is caused by advection and not temporal changes. While the
396 upstream pattern and SPICEcore history cannot be correlated for ages older than 10ka, the spatial
397 pattern is still expected to impact the accumulation history. The dominant timescales affected
398 increase from ~1 ka in the Holocene to ~10 ka at 50 ka age. These timescales are similar to that
399 of millennial climate change and thus, we expect that the coherence between isotopic and
400 accumulation records to be decreased. Overall, changes in accumulation of less than 20% on
401 millennial timescales should not be interpreted as a climate signal.

402

403 The different characters of the advection impact for water isotopes and accumulation arise
404 because there is no coherent relationship between water isotopes and accumulation rate. This
405 may be because the water isotopes are largely controlled by the condensation temperature
406 (Jouzel et al., 1997), whereas the accumulation rate is affected by wind redistribution and the



407 local surface topography (Hamilton, 2004). In fact, the curvature (second derivative) of the
408 elevation profile along the flowline explains a third of the variance in the modern spatial pattern
409 of accumulation, similar to areas in Greenland (Miege et al., 2013; Hawley et al., 2014).

410

411 We could not determine the temperature lapse rate from our 10m borehole temperatures;
412 however, we can estimate the temperature impact of advection based on a dry adiabatic lapse rate
413 of $10^{\circ}\text{C km}^{-1}$, which is consistent with our measurements. The LGM ice fell at 150m higher
414 elevation and likely would be $\sim 1.5^{\circ}$ colder than if it had fallen at the current elevation of South
415 Pole.

416

417 **Conclusion**

418 The relatively fast ice speed at South Pole today causes ice at depth in SPICEcore to have
419 originated at elevations up to $\sim 250\text{m}$ higher and at locations $\sim 150\text{ km}$ away in the direction of
420 Titan Dome. Our measurements in the upstream catchment define the flow direction and speed
421 as well as spatial gradients in the accumulation rate and water isotopes. These measurements
422 identify the non-climate impact of advection on the SPICEcore records. The accumulation rate
423 has no spatial trend, but shows 20% variations on length scales of 5-10km; $\delta^{18}\text{O}$ shows a -
424 0.008‰ m^{-1} depletion which enhances the measured LGM-Holocene change in the ice core by
425 1%. This work facilitates accurate interpretation of the SPICEcore records as temporal histories
426 of climate at a fixed location.

427

428 **Data Availability**

429 Velocity and radar data are available at <http://www.usap-dc.org/view/dataset/601100>. Water
430 isotope, accumulation rate, and advection corrections will be posted upon publication.

431

432 **Author Contributions**

433 All authors contributed to the analysis and writing of the manuscript. HC, DL, MS, and MK
434 performed the field work. AS, TF, and ES performed water isotope analysis.

435

436 **Competing Interests**

437 The authors declare no competing interests.



438

439 **Acknowledgements**

440 This work was funded through U.S. National Science Foundation grants 1443471 and 1443232
441 (MK, EW, HC, TJF); 1443105 and 141839 (EJS). We thank the Ice Drill Program Office for
442 recovering the ice core; the 109th New York Air National Guard for airlift in Antarctica;
443 Elizabeth Morton, David Clemens-Sewall, Maurice Conway, Mike Waskiewicz for their efforts
444 in the field; Antarctic Support Contractors and the members of South Pole station who facilitated
445 the field operations; UNAVCO for power supplies and GPS support; and the National Science
446 Foundation Ice Core Facility for ice core processing.

447

448 **References**

- 449 Alley, R.B., Meese, D.A., Shuman, C.A., Gow, A.J., Taylor, K.C., Grootes, P.M., White, J.W.C.,
450 Ram, M., Waddington, E.D., Mayewski, P.A., and Zielinski, G.A.: Abrupt increase in
451 greenland snow accumulation at the end of the younger dryas event. *Nature*, **362**(6420): 527-
452 529, 1993.
- 453 Briggs, R.D., Pollard, D. and Tarasov, L.: A data-constrained large ensemble analysis of
454 Antarctic evolution since the Eemian. *Quaternary Science Reviews*, **103**: 91-115, 2014
- 455 Casey, K.A., Fudge, T.J., Neumann, T.A., Steig, E.J., Cavitte, M.G.P. and Blankenship, D.D.:
456 The 1500 m South Pole ice core: recovering a 40 ka environmental record. *Annals of*
457 *Glaciology*, **55**(68): 137-146, 2014
- 458 Cuffey, K.M. and Clow, G.D.: Temperature, accumulation, and ice sheet elevation in central
459 Greenland through the last deglacial transition. *Journal of Geophysical Research-Oceans*,
460 **102**(C12): 26383-26396, 1997
- 461 Cuffey, K.M. and Paterson, W.S.B.: *The Physics of Glaciers*. Fourth Edition. 2010
- 462 Dansgaard, W., Johnsen, S.J., Moller, J., Langway Jr., C.C.: One thousand centuries of climatic
463 record from Camp Century on the Greenland Ice Sheet, *Science*, 166, 3903, 377-380, 1969
- 464 DeConto, R.M. and Pollard, D.: Contribution of Antarctica to past and future sea-level rise.
465 *Nature*, **531**(7596): 591-597, 2016
- 466 Dixon, D.A., Mayewski, P.A., Korotkikh, E., Sneed, S.B., Handley, M.J., Introne, D.S. and
467 Scambos, T.A.: Variations in snow and firn chemistry along US ITASE traverses and the
468 effect of surface glazing. *Cryosphere*, **7**(2): 515-535, 2013



- 469 EPICA, Augustin, L., Barbante, C., Barnes, PRF., Barnola, JM., Bigler, M., Castellano, E.,
470 Cattani, O., Chappellaz, J., DahlJensen, D., Delmonte, B., Dreyfus, G., Durand, G., Falourd,
471 S., Fischer, H., Fluckiger, J., Hansson, M.E., Huybrechts, P., Jugie, R., Johnsen, S.J., Jouzel,
472 J., Kaufmann, P., Kipfstuhl, J., Lambert, F., Lipenkov, V.Y., Littot, G.V.C., Longinelli, A.,
473 Lorrain, R., Maggi, V., Masson-Delmotte, V., Miller, H., Mulvaney, R., Oerlemans, J.,
474 Oerter, H., Orombelli, G., Parrenin, .,F Peel, D.A., Petit, J.R., Raynaud, D., Ritz, C., Ruth,
475 U., Schwander, J., Siegenthaler, U., Souchez, R., Stauffer, B., Steffensen, J.P., Stenni, B.,
476 Stocker, T.F., Tabacco, I.E., Udisti, R., van de Wal, R.S.W., van den Broeke, M., Weiss, J.,
477 Wilhelms, F., Winther, J.G., Wolff, E.W., Zucchelli, M.: One-to-one coupling of glacial
478 climate variability in Greenland and Antarctica. *Nature*, **444**(7116): 195-198, 2006
- 479 Fretwell, P., Pritchard, H.D., Vaughan, D.G., Bamber, J.L., Barrand, N.E., Bell, R., Bianchi, C.,
480 Bingham, R.G., Blankenship, D.D., Casassa, G., Catania, G., Callens, D., Conway, H., Cook,
481 A.J., Corr, H.F.J., Damaske, D., Damm, V., Ferraccioli, F., Forsberg, R., Fujita, S., Gim, Y.,
482 Gogineni, P., Griggs, J.A., Hindmarsh, R.C.A., Holmlund, P., Holt, J.W., Jacobel, R.W.,
483 Jenkins, A., Jokat, W., Jordan, T., King, E.C., Kohler, J., Krabill, W., Riger-Kusk, M.,
484 Langley, K.A., Leitchenkov, G., Leuschen, C., Luyendyk, B.P., Matsuoka, K., Mouginot, J.
485 Nitsche, F.O., Nogi, Y., Nost, O.A., Popov, S.V., Rignot, E., Rippin, D.M., Rivera, A.,
486 Roberts, J., Ross, N., Siegert, M.J., Smith, A.M., Steinhage, D., Studinger, M., Sun, B.,
487 Tinto, B.K., Welch, B.C., Wilson, D., Young, D.A., Xiangbin, C. and Zirizzotti, A.:
488 Bedmap2: improved ice bed, surface and thickness datasets for Antarctica. *Cryosphere*, **7**(1):
489 375-393, 2013
- 490 Fudge, T.J., Markle, B.R., Cuffey, K.M., Buizert, C., Taylor, K.C., Steig, E.J., Waddington,
491 E.D., Conway, H. and Koutnik, M.: Variable relationship between accumulation and
492 temperature in West Antarctica for the past 31,000 years. *Geophysical Research Letters*,
493 **43**(8): 3795-3803, 2016
- 494 Golledge, N.R., Menviel, L., Carter, L., Fogwill, C.J., England, M.H., Cortese G., and Levy,
495 R.H.: Antarctic contribution to meltwater pulse 1A from reduced Southern Ocean
496 overturning. *Nature Communications*, **5**, 2014
- 497 Gow, A.J., Ueda, H.T. and Garfield, D.E.: Antarctic ice sheet - preliminary results of first core
498 hole to bedrock. *Science*, **161**(3845): 1011-1014, 1968.
- 499 Hamilton, G.S. 2004. Topographic control of regional accumulation rate variability at South Pole



- 500 and implications for ice-core interpretation. *Annals of Glaciology, Vol 39, 2005*, **39**: 214-218.
- 501 Hammer, C.U., Clausen, H.B., and Dansgaard, W.: Greenland ice-sheet evidence of post-glacial
502 volcanism and its climatic impact. *Nature*, **288**(5788): 230-235, 1980
- 503 Hawley, R.L., Courville, Z.R., Kehrl, L.M., Lutz, E.R., Osterberg, E.C.T., Overly, B. and Wong,
504 G.J.: Recent accumulation variability in northwest Greenland from ground-penetrating radar
505 and shallow cores along the Greenland Inland Traverse. *Journal of Glaciology*, **60**(220): 375-
506 382, 2014
- 507 Huybrechts, P., Rybak, O., Pattyn, F., Ruth, U. and Steinhage, D.: Ice thinning, upstream
508 advection, and non-climatic biases for the upper 89% of the EDML ice core from a nested
509 model of the Antarctic ice sheet. *Climate of the Past*, **3**(4): 577-589, 2007
- 510 Jouzel, J., Alley, R.B., Cuffey, K.M., Dansgaard, W., Grootes, P., Hoffmann, G., Johnsen, S.J.,
511 Koster, R.D., Peel, D., Shuman, C.A., Stievenard, M., Stuiver M., and White, J.: Validity of
512 the temperature reconstruction from water isotopes in ice cores. *Journal of Geophysical*
513 *Research-Oceans*, **102**(C12): 26471-26487, 1997
- 514 Koutnik, M.R., Fudge, T.J., Conway, H., Waddington, E.D., Neumann, T.A., Cuffey, K.M.,
515 Buizert, C., and Taylor, K.C.: Holocene accumulation and ice flow near the West Antarctic
516 Ice Sheet Divide ice core site. *Journal of Geophysical Research-Earth Surface*, **121**(5): 907-
517 924, 2016
- 518 Lilien, D.A., Fudge, T.J., Koutnik, M.R., Conway, H., Osterberg, E.C., Ferris, D.G.,
519 Waddington, E.D. and Stevens, C.M.: Holocene Ice-Flow Speedup in the Vicinity of the
520 South Pole. *Geophysical Research Letters*, **45**(13): 6557-6565: 2018
- 521 Lorius, C., Jouzel, J., Ritz, C., Merlivat, L., Barkov, N.I., Korotkevich, Y.S. and Kotlyakov,
522 V.M.: A 150,000-year climatic record from antarctic ice. *Nature*, **316**(6029): 591-596, 1985
- 523 Marcott, S.A., Bauska, T.K., Buizert, C., Steig, E.J., Rosen, J.L., Cuffey, K.M., Fudge, T.J.,
524 Severinghaus, J.P., Ahn, J., Kalk, M.L., McConnell, J.R., Sowers, T., Taylor, K.C., White,
525 J.W.C., and Brook, E.J.: Centennial-scale changes in the global carbon cycle during the last
526 deglaciation. *Nature*, **514**(7524): 616-620, 2014
- 527 Markle, B.R., Steig, E.J., Buizert, C., Schoenemann, S.W., Bitz, C.M., Fudge, T.J., Pedro, J.B.,
528 Ding, Q.H., Jones, T.R., White, J.C. and Sowers, T. Global atmospheric teleconnections
529 during Dansgaard-Oeschger events. *Nature Geoscience*, **10**(1): 36-40, 2017
- 530 Martinerie, P., Lipenkov, V.Y., Raynaud, D., Chappellaz, J., Barkov, N.I. and Lorius, C.: Air



- 531 content paleo record in the vostok ice core (antarctica) - a mixed record of climatic and
532 glaciological parameters. *Journal of Geophysical Research-Atmospheres*, **99**(D5): 10565-
533 10576, 1994
- 534 Masson-Delmotte, V., Hou, S., Ekaykin, A., Jouzel, J., Aristarain, A., Bernardo, R.T.,
535 Bromwich, D., Cattani, O., Delmotte, M., Falourd, S., Frezzotti, M., Gallee, H., Genoni, L.,
536 Isaksson, E., Landais, A., Helsen, M.M., Hoffmann, G., Lopez, J., Morgan, V., Motoyama,
537 H., Noone, D., Oerter, H., Petit, J.R., Royer, A., Uemura, R., Schmidt, G.A., Schlosser, E.,
538 Simoes, J.C., Steig, E.J., Stenni, B., Stievenard, M., van den Broeke, M.R., de Wal, R., de
539 Berg, W.J.V., Vimeux, F. and White, J.W.C.: A review of Antarctic surface snow isotopic
540 composition: Observations, atmospheric circulation, and isotopic modeling. *Journal of*
541 *Climate*, **21**(13): 3359-3387, 2008
- 542 Miege, C., Forster, R.R., Box, J.E., Burgess, E.W., McConnell, J.R., Pasteris, D.R. and Spikes,
543 V.B.: Southeast Greenland high accumulation rates derived from firn cores and ground-
544 penetrating radar. *Annals of Glaciology*, **54**(63): 322-332, 2013
- 545 Morse, D.L., Blankenship, D.D., Waddington, E.D. and Neumann, T.A. A site for deep ice
546 coring in West Antarctica: results from aerogeophysical surveys and thermo-kinematic
547 modeling. *Annals of Glaciology, Vol 35*, **35**: 36-44, 2002
- 548 NEEM, Dahl-Jensen, D., Albert, M. R., Aldahan, A., Azuma, N., Balslev-Clausen, D.,
549 Baumgartner, M., Berggren, A. -M., Bigler, M., Binder, T., Blunier, T., Bourgeois, J. C.,
550 Brook, E. J., Buchardt, S. L., Buizert, C., Capron, E., Chappellaz, J., Chung, J., Clausen, H.
551 B., Cvijanovic, I., Davies, S. M., Ditlevsen, P., Eicher, O., Fischer, H., Fisher, D. A., Fleet,
552 L. G., Gfeller, G., Gkinis, V., Gogineni, S., Goto-Azuma, K., Grinsted, A., Gudlaugsdottir,
553 H., Guillevic, M., Hansen, S. B., Hansson, M., Hirabayashi, M., Hong, S., Hur, S. D.,
554 Huybrechts, P., Hvidberg, C. S., Iizuka, Y., Jenk, T., Johnsen, S. J., Jones, T. R., Jouzel, J.,
555 Karlsson, N. B., Kawamura, K., Keegan, K., Kettner, E., Kipfstuhl, S., Kjaer, H. A., Koutnik,
556 M., Kuramoto, T., Koehler, P., Laepple, T., Landais, A., Langen, P. L., Larsen, L. B.,
557 Leuenberger, D., Leuenberger, M., Leuschen, C., Li, J., Lipenkov, V., Martinerie, P.,
558 Maselli, O. J., Masson-Delmotte, V., McConnell, J. R., Miller, H., Mini, O., Miyamoto, A.,
559 Montagnat-Rentier, M., Mulvaney, R., Muscheler, R., Orsi, A. J., Paden, J., Panton, C.,
560 Pattyn, F., Petit, J. -R., Pol, K., Popp, T., Possnert, G., Prie, F., Prokopiou, M., Quiquet, A.,
561 Rasmussen, S. O., Raynaud, D., Ren, J., Reutenauer, C., Ritz, C., Rockmann, T., Rosen, J.



- 562 L., Rubino, M., Rybak, O., Samyn, D., Sapart, C. J., Schilt, A., Schmidt, A. M. Z.,
563 Schwander, J., Schuepbach, S., Seierstad, I., Severinghaus, J. P., Sheldon, S., Simonsen, S.
564 B., Sjolte, J., Solgaard, A. M., Sowers, T., Sperlich, P., Steen-Larsen, H. C., Steffen, K.,
565 Steffensen, J. P., Steinhage, D., Stocker, T. F., Stowasser, C., Sturevik, A. S., Sturges, W. T.,
566 Sveinbjornsdottir, A., Svensson, A., Tison, J. -L., Uetake, J., Vallelonga, P., van de Wal, R.
567 S. W., van der Wel, G., Vaughn, B. H., Vinther, B., Waddington, E., Wegner, A., Weikusat,
568 I., White, J. W. C., Wilhelms, F., Winstrup, M., Witrant, E., Wolff, E. W., Xiao, C., Zheng,
569 J.: Eemian interglacial reconstructed from a Greenland folded ice core. *Nature*, **493**(7433):
570 489-494, 2013
- 571 NorthGRIP, Andersen, K.K., Azuma, N., Barnola, J.M., Bigler, M., Biscaye, P., Caillon, N.,
572 Chappellaz, J., Clausen, H.B., DahlJensen, D., Fischer, H., Fluckiger, J., Fritzsche, D., Fujii,
573 Y., Goto-Azuma, K., Gronvold, K., Gundestrup, N.S., Hansson, M., Huber, C., Hvidberg,
574 C.S., Johnsen, S.J., Jonsell, U., Jouzel, J., Kipfstuhl, S., Landais, A., Leuenberger, M.,
575 Lorrain, R., Masson-Delmotte, V., Miller, H., Motoyama, H., Narita, H., Popp, T.,
576 Rasmussen, S.O., Raynaud, D., Rothlisberger, R., Ruth, U., Samyn, D., Schwander, J., Shoji,
577 H., Siggard-Andersen, M.L., Steffensen, J.P., Stocker, T., Sveinbjornsdottir, A.E., Svensson,
578 A., Takata, M., Tison, J.L., Thorsteinsson, T., Watanabe, O., Wilhelms, F., White, J.W.C.:
579 High-resolution record of Northern Hemisphere climate extending into the last interglacial
580 period. *Nature*, **431**(7005): 147-151, 2004
- 581 Parrenin, F., Dreyfus, G., Durand, G., Fujita, S., Gagliardini, O., Gillet, F., Jouzel, J., Kawamura,
582 K., Lhomme, N., Masson-Delmotte, V., Ritz, C., Schwander, J., Shoji, H., Uemura, R.,
583 Watanabe, O. and Yoshida, N. 1-D-ice flow modelling at EPICA Dome C and Dome Fuji,
584 East Antarctica. *Climate of the Past*, **3**(2): 243-259, 2007
- 585 Petit, J.R., Jouzel, J., Raynaud, D., Barkov, N.I., Barnola, J.M., Basile, I., Bender, M.,
586 Chappellaz, J., Davis, M., Delaygue, G., Delmotte, M., Kotlyakov, V.M., Legrand, M.,
587 Lipenkov, V.Y., Lorius, C., Pepin, L., Ritz, C., Saltzman, E. and Stievenard, M.: Climate and
588 atmospheric history of the past 420,000 years from the Vostok ice core, Antarctica. *Nature*,
589 **399**(6735): 429-436, 1999
- 590 Pollard, D. and DeConto, R.M.: Modelling West Antarctic ice sheet growth and collapse
591 through the past five million years. *Nature*, **458**(7236): 329-333, 2009
- 592 Price, S.F., Conway, H., and Waddington, E.D.: Evidence for late pleistocene thinning of Siple



- 593 Dome, West Antarctica. *Journal of Geophysical Research-Earth Surface*, **112**(F3), 2007
- 594 Rignot, E., Mouginot, J., and Scheuchl, B.: Ice Flow of the Antarctic Ice Sheet. *Science*,
- 595 **333**(6048): 1427-1430, 2011
- 596 Severinghaus, J.P., Grachev, A. and Battle, M.: Thermal fractionation of air in polar firn by
- 597 seasonal temperature gradients. *Geochemistry Geophysics Geosystems*, **2**, 2001
- 598 Sodemann, H. and Stohl, A.: Asymmetries in the moisture origin of Antarctic precipitation.
- 599 *Geophysical Research Letters*, **36**, 2009
- 600 Steig, E.J., Ding, Q., White, J.W.C., Kuttel, M., Rupper, S.B., Neumann, T.A., Neff, P.D.,
- 601 Gallant, A.J.E., Mayewski, P.A., Taylor, K.C., Hoffmann, G., Dixon, D.A., Schoenemann,
- 602 S.W., Markle, B.R., Fudge, T.J., Schneider, D.P., Teel, R.P., Vaughn, B.H., Burgener, L.,
- 603 Williams, J., and Korotkikh, E.: Recent climate and ice-sheet changes in West Antarctica
- 604 compared with the past 2,000 years. *Nature Geoscience*, **6**: 372-375, 2013
- 605 Steig, E.J., Fastook, J.L., Zweck, C., Goodwin, I.D., Licht, K., White, J.W.C. and Ackert, R.P.:
- 606 West Antarctic ice-sheet elevation changes. In *Environment of the West Antarctic Ice Sheet*,
- 607 ed. R. Alley and R. Bindshadler, Antarctic Research Series, 75-90, 2001
- 608 Steig, E.J., Kahle, E., Jones, T., Morris, V., Vaughn, B., and White, J., in prep., The SPICEcore-
- 609 triple-isotope record.
- 610 Stenni, B., Buiron, D., Frezzotti, M., Albani, S., Barbante, C., Bard, E., Barnola, J.M., Baroni,
- 611 M., Baumgartner, M., Bonazza, M., Capron, E., Castellano, E., Chappellaz, J., Delmonte, B.,
- 612 Falourd, S., Genoni, L., Iacumin, P., Jouzel, J., Kipfstuhl, S., Landais, A., Lemieux-Dudon,
- 613 B., Maggi, V., Masson-Delmotte, V., Mazzola, C., Minster, B., Montagnat, M., Mulvaney,
- 614 R., Narcisi, B., Oerter, H., Parrenin, F., Petit, J.R., Ritz, C., Scarchilli, C., Schilt, A.,
- 615 Schupbach, S., Schwander, J., Selmo, E., Severi, M., Stocker, T.F. and Udisti, R.: Expression
- 616 of the bipolar see-saw in Antarctic climate records during the last deglaciation. *Nature*
- 617 *Geoscience*, **4**(1): 46-49, 2011
- 618 Veres, D., Bazin, L., Landais, A., Kele, H.T.M., Lemieux-Dudon, B., Parrenin, F., Martinerie, P.,
- 619 Blayo, E., Blunier, T., Capron, E., Chappellaz, J., Rasmussen, S.O., Severi, M., Svensson,
- 620 A., Vinther, B., and Wolff, E.W.: The Antarctic ice core chronology (AICC2012): an
- 621 optimized multi-parameter and multi-site dating approach for the last 120 thousand years.
- 622 *Climate of the Past*, **9**(4): 1733-1748, 2013
- 623 Vinther, B.M., Buchardt, S.L., Clausen, H.B., Dahl-Jensen, D., Johnsen, S.J., Fisher, D.A.,



- 624 Koerner, R.M., Raynaud, D., Lipenkov, V., Andersen, K.K., Blunier, T., Rasmussen, S.O.,
625 Steffensen, J.P. and Svensson, A.M.: Holocene thinning of the Greenland ice sheet. *Nature*,
626 **461**(7262): 385-388, 2009
- 627 Waddington, E.D., Bolzan, J.F. and Alley, R.B.: Potential for stratigraphic folding near ice-sheet
628 centers. *Journal of Glaciology*, **47**(159): 639-648, 2001
- 629 Waddington, E.D., Conway, H., Steig, E.J., Alley, R.B., Brook, E.J., Taylor, K.C. and White,
630 J.W.C.: Decoding the dipstick: Thickness of Siple Dome, West Antarctica, at the Last Glacial
631 Maximum. *Geology*, **33**(4): 281-284, 2005
- 632 Waddington, E.D., Neumann, T.A., Koutnik, M.R., Marshall, H.P., and Morse, D.L.: Inference
633 of accumulation-rate patterns from deep layers in glaciers and ice sheets. *Journal of*
634 *Glaciology*, **53**(183): 694-712, 2007
- 635 Whillans, I.M., Jezek, K.C., Drew, A.R. and Gundestrup, N.: Ice flow leading to the deep core
636 hole at dye-3, greenland. *Annals of Glaciology*, **5**: 185-190, 1984
637